AFRL-RZ-WP-TP-2012-0126

TIME-RESOLVED MAGNETO-OPTICAL IMAGING OF $Y_1Ba_2Cu_3O_{7-\delta}$ THIN FILMS IN HIGH-FREQUENCY AC CURRENT REGIME (POSTPRINT)

A. Lucarelli and G. Lüpke

The College of William and Mary

T.J. Haugan, G.A. Levin, and P.N. Barnes

Mechanical Energy Conversion Branch
Energy/Power/Thermal Division

FEBRUARY 2012

AIR FORCE RESEARCH LABORATORY
PROPULSION DIRECTORATE
WRIGHT-PATTERSON AIR FORCE BASE, OH 45433-7251
AIR FORCE MATERIEL COMMAND
UNITED STATES AIR FORCE

REPORT DOCUMENTATION PAGE

Form Approved
OMB No. 0704-0188

1. REPORT DATE *(DD-MM-YY)*	2. REPORT TYPE	3. DATES COVERED *(From - To)*
February 2012	Journal Article Postprint	01 January 2004 – 01 January 2006

4. TITLE AND SUBTITLE

TIME-RESOLVED MAGNETO-OPTICAL IMAGING OF $Y_1Ba_2Cu_3O_{7-\delta}$ THIN FILMS IN HIGH-FREQUENCY AC CURRENT REGIME (POSTPRINT)

5a. CONTRACT NUMBER
In-house

5b. GRANT NUMBER

5c. PROGRAM ELEMENT NUMBER
62203F

6. AUTHOR(S)

A. Lucarelli and G. Lüpke (College of William and Mary)
T.J. Haugan, G.A. Levin, and P.N. Barnes (AFRL/RZPG)

5d. PROJECT NUMBER
3145

5e. TASK NUMBER
32

5f. WORK UNIT NUMBER
314532ZE

7. PERFORMING ORGANIZATION NAME(S) AND ADDRESS(ES)

The College of William and Mary
Department of Applied Science
Williamsburg, VA 23187-8795

Mechanical Energy Conversion Branch (AFRL/RZPG)
Energy/Power/Thermal Division
Air Force Research Laboratory, Propulsion Directorate
Wright-Patterson Air Force Base, OH 45433-7251
Air Force Materiel Command
United States Air Force

8. PERFORMING ORGANIZATION REPORT NUMBER
AFRL-RZ-WP-TP-2012-0126

9. SPONSORING/MONITORING AGENCY NAME(S) AND ADDRESS(ES)

Air Force Research Laboratory
Propulsion Directorate
Wright-Patterson Air Force Base, OH 45433-7251
Air Force Materiel Command
United States Air Force

10. SPONSORING/MONITORING AGENCY ACRONYM(S)
AFRL/RZPG

11. SPONSORING/MONITORING AGENCY REPORT NUMBER(S)
AFRL-RZ-WP-TP-2012-0126

12. DISTRIBUTION/AVAILABILITY STATEMENT

Approved for public release; distribution unlimited.

13. SUPPLEMENTARY NOTES

Journal article published in *Superconductor Science and Technology*, Vol. 19, 2006.

 Work on this effort was completed in 2006.

PA Case Number: AFRL/WS 06-0233; Clearance Date: 06 Dec 2006.

14. ABSTRACT

We present a time-resolved magneto-optical (MO) imaging study of high-temperature superconductor (HTS) in a high-frequency alternating current (AC) regime. The evolution of the magnetic flux density distribution in $YBa_2Cu_3O_{7-\delta}$ (YBCO) thin film samples is studied as a function of the phase of the applied AC current. A quantitative analysis of the data shows that the maxima of the AC current density is shifted from the edges further inside the sample, which may be caused by the higher self-induced field in that region. This technique can be used to study magnetic flux evolution in HTS films and coated conductors in the high-frequency current regime.

15. SUBJECT TERMS

time-resolved magneto-optical, imaging study, high-temperature superconductor, magnetic flux density, thin film samples

16. SECURITY CLASSIFICATION OF:			17. LIMITATION OF ABSTRACT:	18. NUMBER OF PAGES	19a. NAME OF RESPONSIBLE PERSON (Monitor)
a. REPORT	b. ABSTRACT	c. THIS PAGE			Timothy J. Haugan
Unclassified	Unclassified	Unclassified	SAR	10	19b. TELEPHONE NUMBER *(Include Area Code)* N/A

INSTITUTE OF PHYSICS PUBLISHING SUPERCONDUCTOR SCIENCE AND TECHNOLOGY

Supercond. Sci. Technol. **19** (2006) 667–670 doi:10.1088/0953-2048/19/6/041

Time-resolved magneto-optical imaging of $Y_1Ba_2Cu_3O_{7-\delta}$ thin films in high-frequency AC current regime

A Lucarelli[1], G Lüpke[1], T J Haugan[2], G A Levin[2] and P N Barnes[2]

[1] Department of Applied Science, The College of William and Mary, Williamsburg, VA 23187-8795, USA

[2] Air Force Research Laboratory, Wright-Patterson AFB, OH 45433-7919, USA

Received 13 February 2006, in final form 28 March 2006
Published 9 May 2006
Online at stacks.iop.org/SUST/19/667

Abstract

We present a time-resolved magneto-optical (MO) imaging study of high-temperature superconductor (HTS) in a high-frequency alternating current (AC) regime. The evolution of the magnetic flux density distribution in $YBa_2Cu_3O_{7-\delta}$ (YBCO) thin film samples is studied as a function of the phase of the applied AC current. A quantitative analysis of the data shows that the maxima of the AC current density is shifted from the edges further inside the sample, which may be caused by the higher self-induced field in that region. This technique can be used to study magnetic flux evolution in HTS films and coated conductors in the high-frequency current regime.

High-temperature superconducting (HTS) rotating machines and transformers, have the potential to deliver electrical power in smaller, lighter, and more efficient systems [1–3]. These important applications involve alternating currents (AC) with frequencies in the range of 10–1000 Hz. The alternating magnetic fields associated with these applications can result in significant AC losses in the superconductor. However, these losses can be considerably reduced by adopting a filamentary geometry [4], as recently demonstrated in a filamentized coated conductor [4–6]. Losses in HTS conductor architecture can be further reduced by adopting additional AC-tolerant measures [2, 7–9]. In the HTS layer, the adjacent normal metal (such as the stabilizer and substrate), and interfilamentary barriers, the AC losses are determined by the spatio-temporal behaviour of the magnetic vortices moving in response to the time-varying magnetic field either applied and/or resulting from the transport current.

Currently, most estimates of the losses in superconductors rely on a nonlinear relationship between the current density and electric field $\vec{E} = \rho(|\vec{j}|)\vec{j}$ and assume that the temperature is fixed [7]. This implies that the induced electric field responsible for the losses changes on the same time scale as the applied magnetic field. However, recent investigations of the low-temperature superconductors reveal a much more intricate picture of flux penetration into a superconductor [10, 11]. Flux jumps were observed that lead to dendritic avalanches developing over time scales much shorter than those determined by the ramping rate of the applied field. This phenomenon may be important for applications. As a result of the highly nonequilibrium pattern of flux penetration, the amount of losses in composite superconductors such as copper stabilized coated YBCO conductors may greatly exceed the traditional estimates.

In order to determine whether the nonequilibrium pattern formation takes place in practical superconductors operating in cyclic regime in the frequency range 10–10^3 Hz, it is necessary to use measurement techniques with inherent time and spatial resolution capable of studying the dynamics of fluxons in a large area. A time-resolved magneto-optical (MO) imaging technique would be particularly effective due to the advantages of being both quantitative and fast.

We developed a time-resolved MO imaging technique to study HTS samples in the high-frequency AC current regime. Our experimental setup, sketched in figure 1, consists of a custom assembled Olympus polarizing microscope combined with a Janis ST-500 continuous-flow cryostat with an operating range of 3.5–325 K with a 50 mK stability. The cryostat has been specifically adapted to mount a permanent magnet or electromagnetic coil around a cold finger. A 0.4 mm thick sapphire window on top of the cryostat allows optical access to the sample. A 10× fluorite tension-free objective lens is used to minimize depolarization effects. A Glan–Thompson polarizer in combination with a linear polarizer provides an extinction ratio of approximately 10^{-5}. For

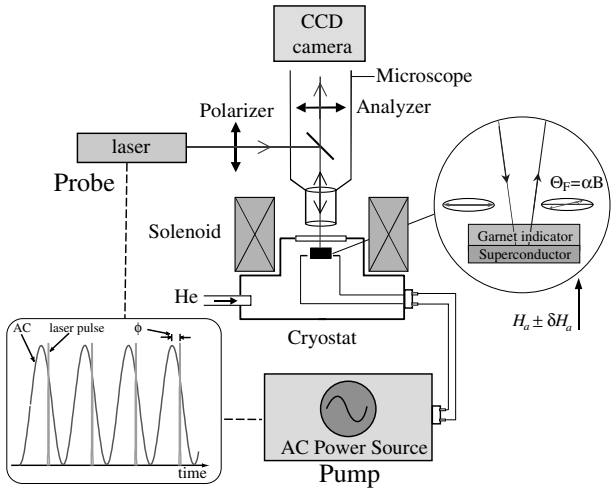

Figure 1. Schematic diagram of the time-resolved MO imaging setup.

time-resolved imaging, we use a Q-switched Nd:YLF diode-pumped solid-state laser which provides 100 ns short pulses at 527 nm wavelength. The pulse repetition frequency (PRF) of the laser can be varied from single shot to 1200 Hz by an externally triggered Pockels cell. We synchronize the laser PRF to the AC current frequency generated by a computer controlled power source in order to obtain time-resolved MO images of the current flow in the sample. We use a 6 μm thick epitaxial grown ferrite-garnet film (FGF) $(Y, Bi, Pr, Lu)_{3.0}(Fe, Ga)_{5.0}O_{12.0}$ with an in-plane magnetization as the MO indicator which is mounted on top of the HTS sample [12]. The iron garnet, shown in the inset of figure 1, shows a pronounced Faraday rotation of about 1.08° μm^{-1} for an external magnetic field of 750 Oe perpendicular to the film surface. Currently, the time resolution of our setup is determined by the jitter (<1 μs) in the synchronization between the PRF and the AC current. Ultimately the time resolution achievable with this method will be limited to sub-nanoseconds by the magnetization switching time of the FGF as in [13].

The power source provides up to 15 A of bipolar current in a customizable waveform at frequencies from 15 to 1200 Hz. Time-resolved images of the magnetic flux distribution in the superconducting sample are collected by a deep cooled charge-coupled device (CCD) camera. The camera has a 12 bit dynamic range grey scale with excellent linearity and low dark current of 0.03 electron/pixel/s. The effective area of the camera is 8.67 mm × 6.60 mm consisting of 1344 × 1024 square format pixels, 6.45 μm in width. The camera which has a minimum exposure time of 10 μs is interfaced to a PC which acquires the images at a frame rate of 8.8 frames s^{-1}.

The YBCO samples were grown by pulsed laser deposition on a $LaAlO_3$ or $SrTiO_3$ substrate with typical dimensions of 10 mm × 5 mm [14]. The YBCO films are about 250 nm thick. The samples exhibit a critical transition temperature (T_c) of ~91 K, as determined by AC susceptibility measurements, and show a sharp transition within two degrees (at 2.2 Oe loss data). The samples are bridged using a photolithographic technique with a length of 6 mm and a cross-section $2w = 475$ μm to reduce their critical current. Transport current measurements show a critical current density $J_c \sim 3$ MA cm^{-2} for the samples at 77 K.

In the MO imaging experiments, the YBCO sample is first cooled to the superconducting state down to 25 K in zero external field, and then an external magnetic field of $B_a = 30$ mT is applied normal to the plane of the sample (z-direction). An AC current $I(t) = I_0 \sin(2\pi f \cdot t)$ is sent through the bridge of the sample (y-direction) and time-resolved MO images are taken at discrete values of the phase angle $\phi = 2\pi f \cdot t$. This is accomplished through an adjustable electronic time delay between the laser pulses and the applied AC current (inset of figure 1). An image with a good contrast requires an exposure time which covers ten laser pulses. Thus the exposure time of the camera is adjusted according to the frequency of the AC current. Figure 2 displays three time-resolved MO images taken at $f = 400$ Hz and $I_{rms} = 5$ A for different values $\phi = -\pi/2, 0, \pi/2$. The white arrows in the images indicate the direction of the current. The sample shows flux profiles with a large self-field at the sample edges indicated by the bright vertical lines and a monotonically decreasing flux density towards the sample interior that reaches the minimum value slightly beyond $w/2$ on both sides. At the sample edges the occurrence of zigzag lines is more pronounced because the gradient of the magnetic field is higher. These lines originate from Bloch walls separating different magnetic domains in the FGF. This flux profile includes finger-like patterns with an average width of approximately 50 μm and a length of about 100 μm corresponding to the flux front. The high-magnification images also reveal small defects present on the surface of the MO indicator, such as the thin line close to the middle of the right edge and a few dark spots.

The images shown in figure 2 have been carefully calibrated to obtain a quantitative analysis of the measured intensities following the procedure described in [13]. The corresponding cross-sectional profiles, shown in the bottom part of figure 2, represent averages along the y-direction for the length of the image. The absolute maximum of the magnetic flux density alternates between the right and left edges of the sample as the phase ϕ changes from $-\pi/2$ to $+\pi/2$ at a rate of 400 Hz, respectively. The magnetic flux profile peaks clearly inside the sample on the side opposite to the absolute maximum and forms a dip at the sample edge, which is more pronounced for $\phi = -\pi/2$. For the intermediate value $\phi = 0$, the penetration of the magnetic flux lines is almost symmetric across the sample and both maxima are very close to the sample edges. The intensity and the position of both peaks of the flux profiles change considerably with the phase. However, the flux front penetration remains almost unchanged in the phase evolution, in contrast to what the critical state model would predict [15]. Similar anomalies have been observed in pulsed current measurements [16] and have been attributed to the presence of relaxation effects due to flux creep in the sample. Figure 3 presents the current-density distributions in the cross-section of the bridge (x-direction) for different values of the phase ϕ. The curves are calculated from the measured flux-density distribution shown in figure 2 using a one-dimensional inversion scheme [13]. The normal component (z-direction) of the magnetic field at a distance h above the sample is related to

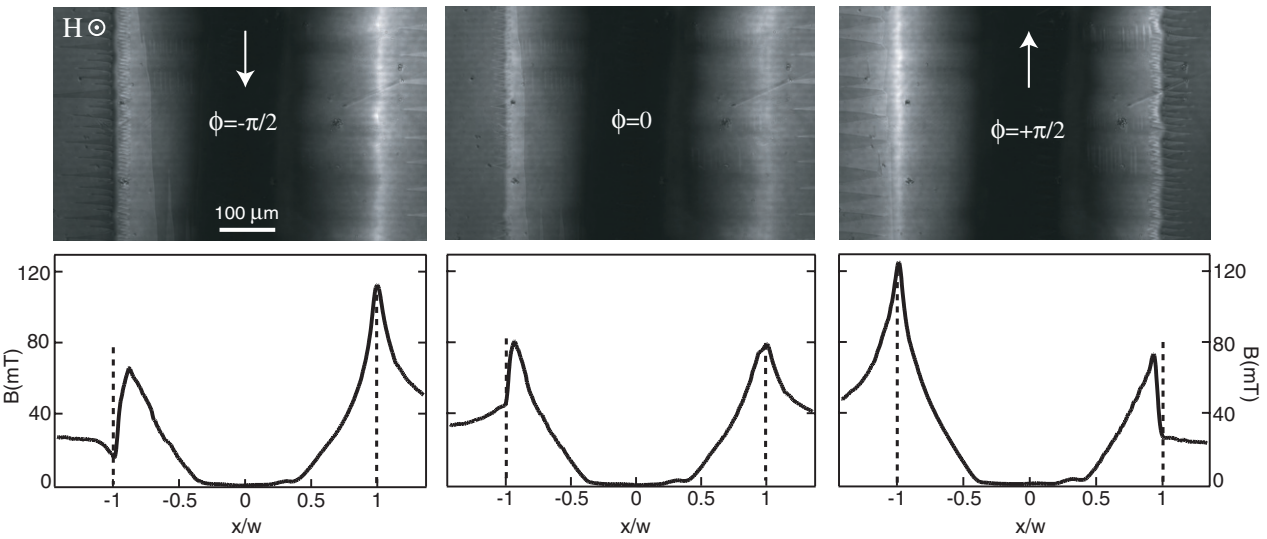

Figure 2. Time-resolved MO images for different values of the phase ϕ of the applied AC current. The white arrow in the images indicates the current direction. The applied magnetic field is applied normal to the film surface. The dashed lines represent the sample edges.

the current-density distribution by Biot–Savart's law:

$$B(x) = B_a + \frac{\mu_0}{2\pi}\int_{-\frac{w}{2}}^{\frac{w}{2}} dx' \frac{x'-x}{h^2+(x'-x)^2} J(x'). \qquad (1)$$

The inversion of this equation then gives the current density profile, $J(x)$, across the bridge, which is expressed by the discrete formula [13]:

$$J(n) = \sum_{n'} \frac{n-n'}{\mu_0 \pi}\left(\frac{1-(-1)^{n-n'}\,e^{\pi d}}{d^2+(n-n')^2} + \frac{[d^2+(n-n')^2-1][1-(-1)^{n-n'}\,e^{\pi d}]}{[d^2+(n-n'+1)^2][d^2+(n-n'-1)^2]}\right) \qquad (2)$$

where $x = \Delta/n$, Δ is the measurement step used for the discretization of the data, $d = h/\Delta$ and $h \cong 10\ \mu$m (approximate distance between MO indicator and HTS sample). This formula includes a Hanning window filtering function to smooth high-frequency signals originating from sources other than the current in the sample. However, since the high-k components are suppressed by this inversion procedure, the accuracy of $J(x)$ near the sample edge can be improved using the iteration procedure suggested in [16]. $J_N(x)$, calculated on the Nth iteration step, is set equal to zero outside the superconductor and substituted into equation (1) to get the flux distribution $B_N(x)$. The difference $B(x) - B_N(x)$ is then substituted into equation (2) to calculate $\delta J_N(x)$. We then set $J_{N+1}(x) = J_N(x) + \delta J_N(x)$ and start the next iteration. Few iterations result in a sharper profile close to zero near the sample edges. Integration of the calculated current density for $\phi = -\pi/2$ and $+\pi/2$ gives $I = 6.9$ and 10.2 A, respectively, indicating reasonable agreement with the applied peak current of 7.1 A. The slightly asymmetric current density profile at $\phi = 0$ is due to the uncertainty in determining the zero phase with the synchronization circuitry.

The value of the critical current density J_c at 25 K can be estimated by taking the maximum absolute value of the current density profile plotted in figure 3. For both phases, $\phi = -\pi/2$ and $+\pi/2$, J_c corresponds to 4.5×10^{11} A m^{-2}. This value is

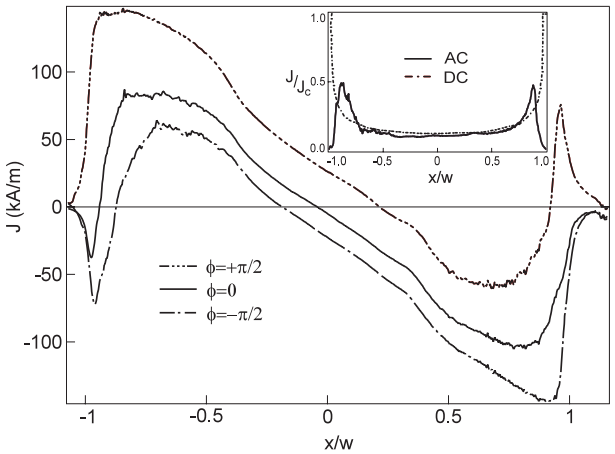

Figure 3. Current density profiles for different values of the phase. The solid curve in the inset shows the difference in AC current density profiles between $\phi = -\pi/2$ and 0. The dashed line represents the calculated DC current profile adapted from [15].

in good agreement with the $J_c = 4.1 \times 10^{11}$ A m^{-2} estimated for this film from the J_c temperature dependence of a reference YBCO film measured by the vibrating sample magnetometry (VSM) method [14].

The current density profiles change considerably with the phase. For example, when $\phi = 0$ there is no net current flowing through the sample, and only the shielding superconducting current flows in a closed loop near the sample edges. At different values of the phase an external current flows through the sample in the positive or negative y-direction according to the polarity of the applied AC voltage. The inset of figure 3 shows the difference (solid curve) in the AC current density profiles between $\phi = 0$ and $-\pi/2$. This is a useful method to distinguish between applied and screening currents. The dotted curve in the inset of figure 3 (adapted from [15]) represents the current profile calculated for a DC current of 0.2 J_C which is comparable to the current in our measurement. The comparison of the two curves shows that the maxima of the

AC current density are shifted from the edges further inside the sample, in contrast to the DC current profile where the current density reaches the critical value close to the edges. This behaviour is also revealed by the AC current density profiles shown in figure 3. In this case, the critical current is reduced at the edges due to the higher self-induced magnetic field in that region, as explained by recent calculations [17, 18]. A more detailed study of the phase and frequency dependence of the AC current profile is necessary to elucidate more precisely the observed effect and the role of the self-induced field.

AC losses in YBCO films have been studied recently in a perpendicular magnetic field [19] and the results have been described by theories based on the Bean critical model incorporating the field-dependent critical-current densities [20]. These studies were done only at 20 and 30 Hz with no spatial or temporal resolution. In the presence of a ramping field, the thermal and magnetic instabilities can cause dramatic changes in the flux penetration that can occur on different time and length scales. A detailed series of measurements of the AC current density in small increments of the phase angle and frequency could reveal which relaxation mechanism governs the current dissipation in HTS conductor.

In summary, we showed how a time-resolved MO imaging technique can be used to study AC currents in HTS samples in the high-frequency regime. Time and spatially-resolved images of the magnetic flux profiles in a thin film YBCO sample are presented for different values of the phase. A quantitative analysis of the data allows us to calculate the current density profiles at different phase angles and to isolate the contribution of applied AC current from the screening current due to the static magnetic field. We observe a sizable shift of the maxima of the AC current density from the edges of the sample, which we attribute to the higher self-induced magnetic field in that region. The presented MO imaging technique can be used to study magnetic flux evolution in the high-frequency current regime.

Acknowledgment

The work at CWM is supported in part by DOE grant DE-FG02-04ER46127.

References

[1] Kalsi S S, Weeber K, Takesue H, Lewis C, Neumueller H W and Blaugher R D 2004 *Proc. IEEE* **92** 1688
[2] Barnes P N, Sumption M D and Rhoads G L 2005 *Cryogenics* **45** 670
[3] Barnes P N, Rhoads G L, Tolliver J C, Sumption M D and Schmaeman K W 2005 *IEEE Trans. Magn.* **41** 268–73
[4] Carr W J Jr and Oberly C E 1999 *IEEE Trans. Appl. Supercond.* **9** 1475–8
[5] Cobb C B, Barnes P N, Haugan T J, Tolliver J, Lee E, Sumption M, Collings E and Oberly C E 2002 *Physica* C **382** 52–6
[6] Amemiya N, Kasai S, Yoda K, Jiang Z, Levin G A, Barnes P N and Oberly C E 2004 *Supercond. Sci. Technol.* **17** 1464
[7] Carr W J Jr 2001 *AC Loss and Macroscopic Theory of Superconductors* 2nd edn (London: Taylor and Francis) and references therein
[8] Sumption M D, Collings E W and Barnes P 2005 *Supercond. Sci. Technol.* **18** 122
[9] Levin G A, Barnes P N, Amemiya N, Kasai S, Yoda K and Jiang Z 2005 *Appl. Phys. Lett.* **86** 072509
[10] Aranson I S *et al* 2005 *Phys. Rev. Lett.* **94** 037002 and references therein
[11] Rudnev I A *et al* 2005 *Appl. Phys. Lett.* **87** 042502 and references therein
[12] Helseth L E, Hansen R W, Il'yashenko E I, Baziljevich M and Johansen T H 2001 *Phys. Rev.* B **64** 174406
[13] Jooss Ch, Albrecht J, Kuhn H, Leonhardt S and Kronmuller H 2002 *Rep. Prog. Phys.* **65** 651–788
[14] Haugan T, Barnes P N, Maartense I, Cobb C B, Lee E J and Sumption M 2003 *J. Mater. Res.* **18** 2618
[15] Zeldov E, Clem J R, McElfresh M and Darwin M 1994 *Phys. Rev.* B **49** 9802
[16] Bobyl A V, Shantsev D V, Galperin Y M, Johansen T H, Baziljevich M and Karmanenko S F 2002 *Supercond. Sci. Technol.* **15** 82–9
[17] Stavrev S, Grilli F, Dutoit B and Ashworth S P 2005 *Supercond. Sci. Technol.* **18** 1300–12
[18] Babaei Brojeny A A and Clem J R 2005 *Supercond. Sci. Technol.* **18** 888–95
[19] Suenaga M *et al* 2003 *J. Appl. Phys.* **94** 502
[20] Shantsev D V, Galperin Y M and Johansen T H 2000 *Phys. Rev.* B **61** 9699